

Synthetic Strategy for the Development of Conjugated Polyelectrolytes as Cathode Interfacial Layers: Toward Sustainable Organic Devices

Mariacecilia Pasini,* Francesco Galeotti,* Wojciech Mróz, Benedetta Maria Squeo, Silvia Luzzati, Chiara Botta, Guido Scavia, and Umberto Giovanella*

The use of conjugated polyelectrolytes (CPEs) as interfacial layers (ILs) to increase the efficiency of organic light-emitting diodes (OLEDs), organic solar cells (OSCs), and organic transistors is a well-established strategy. Here, the rational process is reported that led to develop the bifunctional poly[(2,7-(9,9'-bis(6'-diethoxyphosphorylhexyl)-fluorene)-alt-(2,7-(9,9'-bis(6'-trimethylammonium bromide)hexyl)-fluorene)] (PF-NBr-EP). PF-NBr-EP is successfully incorporated as a cathode IL (CIL) in diverse electronic and optoelectronic devices. The properties of two fluorene-based CPEs containing, respectively, phosphonate (EP) and ammonium (NBr) moieties used as building blocks for the synthesis of the PF-NBr-EP copolymer and their mixtures are investigated to evaluate the combined effect of the two moieties and therefore to gain insight into the behavior of PF-NBr-EP chemical structure in the devices. Additionally, the performance of OLEDs and OSCs is analyzed based on established active layers, incorporating all these neat and mixed CILs.

solvents, which may cause erosion of the subsequent layers during multilayer integration. Many efforts have been devoted to overcome this problem.^[3] Particularly interesting are materials comprising a π -conjugated backbone with pendant polar or ionic groups that are processable from water or alcohol, i.e., environmental-friendly solvents, since they offer great opportunities to avoid interfacial mixing upon fabrication of multilayer organic optoelectronic devices by low-cost solution methods.^[4]

Among them, CPEs combine tunable functional properties and match with the growing demand for eco-friendly materials and sustainable synthetic routes.

Literature examples of CPEs used in OSCs or LEDs proved their ability mainly as a CIL to improve charge extraction/injection to/from low work-function metal cathode, resulting in devices performance.^[5–7]

However, each type of device or active layer usually requires a specific CPE to work properly, while the development of CPEs suitable as CILs for as broad as possible types of both active layers and devices has been rarely achieved.

Among promising CPEs reported in the literature, the most fascinating are those with a backbone belonging to polyfluorenes (PFs) family.^[8–14] The reason relies on the easy functionalization of the fluorenic monomer in the 9,9' positions with alkyl halides and on the use of Suzuki coupling that is compatible with various functional groups and can be carried out in aqueous solvents.^[15] Moreover, from an optical point of view, PF films are practically colorless and this makes it possible to use them in multilayer devices without affecting optical properties of the active layers.


The choice of functional group determines the main CPE action. Literature data indicate that the phosphonate (EP) functionality may have an effective role in the stabilization of the metal contact,^[16,17] while the ammonium functionality (NBr) can form dipoles that modify the charge injection/extraction barriers at the organic/cathode electrode interface,^[13,18–20] for both OPVs and OLEDs.^[6,21,22] Additionally, in polymer:fullerene solar cells the NBr moiety can improve interfacial contacts and reduce transport loss upon doping the fullerene component close to the IL.^[23]

1. Introduction

Electrode interfacial engineering is a widely adopted strategy to maximize the performances of organic optoelectronic devices, such as OLEDs and OSCs.^[1,2] Further, it becomes even more important in the case of solution-processed devices where a multilayer architecture is often critical to achieve.

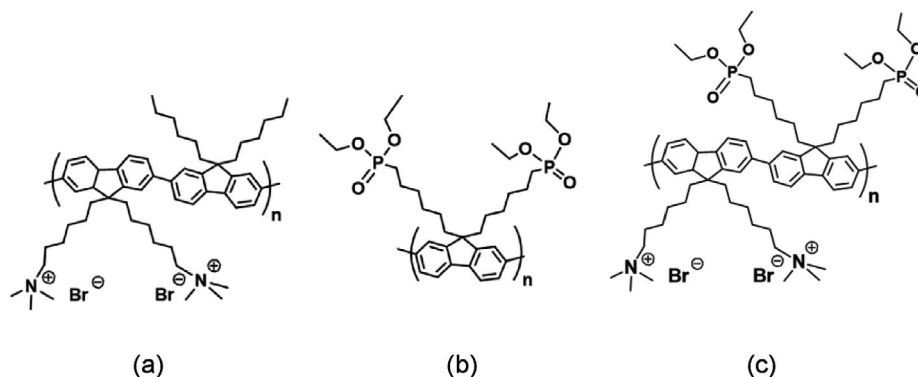
In fact, most of the commonly used emissive and charge transport materials have similar solubility in common organic

M. Pasini, F. Galeotti, W. Mróz, B. M. Squeo, S. Luzzati, C. Botta, G. Scavia, U. Giovanella
 National Research Council (CNR)
 Institute of Chemical Sciences and Technologies “G. Natta” (SCITEC)
 via A. Corti 12, Milan 20133, Italy
 E-mail: mariacecilia.pasini@scitec.cnr.it; francesco.galeotti@scitec.cnr.it; umberto.giovanella@cnr.it

 The ORCID identification number(s) for the author(s) of this article can be found under <https://doi.org/10.1002/macp.202300130>

© 2023 The Authors. Macromolecular Chemistry and Physics published by Wiley-VCH GmbH. This is an open access article under the terms of the Creative Commons Attribution License, which permits use, distribution and reproduction in any medium, provided the original work is properly cited.

DOI: 10.1002/macp.202300130



Scheme 1. Chemical structure of a) P1, b) P2, and c) PF-NBr-EP CPEs.

With this in mind, we recently developed a poly[(2,7-(9,9'-bis(6'-diethoxyphosphorylhexyl)fluorene)-alt-(2,7-(9,9'-bis(6''-trimethylammonium bromide)hexyl)fluorene)] (PF-NBr-EP, **Scheme 1c**) composed of fluorene units having as an alternating terminal group of the alkyl side chains, the EP or the NBr groups, and successfully used it as a CIL to boost efficiencies of diverse electronic and optoelectronic devices such as organic and nanocrystal-based LEDs,^[24,25] OSCs,^[26] organic light-emitting transistors (OLETs).^[27] PF-NBr-EP is easily processable in either water, ethanol or methanol, with a good compatibility with different active layers. Moreover, its successful use relies on its electron charge selectivity and/or minimized energy barrier to the cathode achieved by tuning film thickness.

In this work we show the rational process that led us to develop the bifunctional PF-NBr-EP interlayer. Specifically, two polar fluorene-based polymers have been taken into consideration, one containing the NBr group as a terminal unit of the side chains and one containing the EP group.^[12,18,28] In both cases the polar/ionic functionalities are obtained with a post polymerization reaction. In fact, the polymers containing the Br-end groups on the alkyl side chains are synthesized and subsequently functionalization is carried out as reported in the literature.^[25,27]

The properties of the two polymer films and of their mixtures in different ratios are investigated to explain the electronic characteristics of PF-NBr-EP and its successful application in devices. Additionally, we analyzed the performance of OLEDs and OSCs, based on established polymeric active layers (Figure S2, Supporting Information), incorporating all these neat and mixed CILs, in comparison to the corresponding PF-NBr-EP-based devices.

2. Results and Discussion

2.1. Synthesis

Among the alcohol-soluble π -conjugated polymers used for interfacial engineering, Poly[(2,7-(9,9'-dioctyl)fluorene)-alt-(2,7-(9,9'-bis(6''-trimethylammonium bromide)hexyl)fluorene)] (hereafter P1, **Scheme 1a**) is one of the most studied and finds application in different device configurations. In fact, quaternary ammonium bromide group has been reported to be effective in re-arranging the organic/cathode electrode energy levels, with a beneficial effect on both OSC and OLED devices.^[13,18,19,29] Poly[9,9-bis(6'-diethoxyphosphorylhexyl)fluorene] (hereafter P2, **Scheme 1b**), on the other hand, is a neutral π -conjugated polymer that, thanks

to the presence of the EP groups, was reported to be able not only to modify the electrode work function but also to exhibit a strong interaction with Aluminum.^[16] This specific feature was shown to favor charge injection and device stability in OLEDs devices as well as to enhance the efficiency of OSCs.^[26] P1 and P2 were synthesized according to the literature.^[25,27]

The PF-NBr-EP polymer was designed to incorporate both these functionalities. PF-NBr-EP was synthesized (**Scheme 1**, Supporting Information) as reported in our previous paper^[24] starting from the monomers 2,7-bis-[9,9'-bis(6''-bromohexyl)fluorenyl]-4,4,5,5-tetramethyl[1,3,2]dioxaborolane and 2,7-dibromo-9,9-bis(6'-diethoxyphosphorylhexyl)fluorene. The cationic polymer was obtained by trimethylamine ionization of the neutral precursor, referring to a reported procedure.^[25]

Before developing a polymer containing both moieties, it was necessary to understand whether their contribution to the functioning of the devices could be effectively complementary with a greater beneficial effect than the use of the single ones.

Therefore, we investigated this point by blending P1 and P2 in three different ratios (**Table 1**) and by analyzing the relationship between the blend composition and the properties of interest of the devices.

2.2. Optical and Morphological Characterization

CPEs exhibit a good solubility in protic polar solvents with uniform film forming properties that allows the deposition from EtOH solution for the optical and morphological characterization.

Contact angles (**Figure 1a**) of a water drop of 2 μ L deposited on the film surface, and instantly measured, show that P1 is hydrophobic while P2 is very hydrophilic (**Figure S1**, Supporting

Table 1. Details of the composition of the blends used as CIL.

	CPEs ratios	
	P1	P2
CIL1	1	0
CIL2	1	0.5
CIL3	1	1
CIL4	1	2
CIL5	0	1

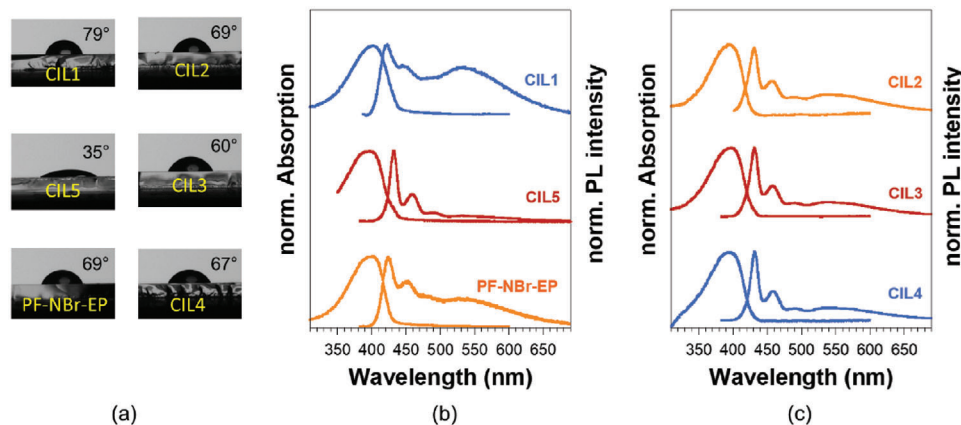


Figure 1. a) Images of water drop deposited on CIL film surfaces and corresponding average contact angles. Absorption and PL spectra (vertically shifted for clarity, excitation at 375 nm) of b) CIL1,5 and c) CIL2-4 spin-coated on quartz substrates. PL spectrum of PF-NBr-EP film is reported as reference.

Information). Blends and PF-NBr-EP show comparable hydrophilicity.

Absorption spectra of films are similar for all CILs and show a main band peaked at 395 nm typical of polyfluorenes (Figure 1b,c). Photoluminescence (PL) spectra of CIL1-5 films (Figure 1b,c), recorded by exciting at 375 nm, exhibit typical fluorene features with peaks at 423–433, 446–458 nm, accompanied by green emission band (centered at ≈ 540 nm) most likely associated to partial oxidation (the keto-defect emission).^[30]

In general, the content of keto-defect does not affect neither the energy levels of the fluorene-based CPE^[26] nor its absorption spectrum. However, the contribution of keto-defect to the PL emission is apparently marked (mainly in CIL1), because it's enhanced by resonant energy transfer that takes place in solid-state from excited fluorene moieties to oxidized states.^[31] In the following this contribution can be neglected since these polymers are not involved in the emission process, and keto-defects do not influence photovoltaic performance.^[28]

2.3. Optoelectronic Devices

We prepared and characterized multi-layered OLED and OSC prototypes with a conventional geometry (direct configuration)^[32] and established active layers (ALs, Figure S2, Supporting Information) to show the advantages of the incorporation of the CIL based on P1 and P2 and their mixtures (CIL1-5), and to compare the results to the devices with PF-NBr-EP used as CIL.

The thickness of CILs is a very critical parameter that heavily influences the device performance. Moreover, different types of devices, i.e., OLEDs and OSCs, due to their peculiar working mechanisms, need different optimized CIL thickness. Therefore, by tuning solution concentration and spin-coating process parameters, we prepared CILs films with two precise thicknesses: OLEDs incorporate a 20 nm thick film of CILs while for OSCs it was reduced to 5 nm.^[26,33]

2.3.1. OLEDs

Polymers P1, P2 and their blends were tested as a CIL in OLEDs (Figure 2a) based on a red-emitting layer con-

sisting of a mixture PVK:PBD:IrRE, where PVK stands for poly(9-vinylcarbazole), PBD means 2-(4-biphenyl)-5-(4-tert-butylphenyl)-1,3,4-oxadiazole and IrRE is the iridium complex with bis(2-(9,9-dibutylfluorenyl)-1-isoquinoline(acetylacetonate) ligand (Figure S2, Supporting Information). All these compounds are commercially available, easy processable, and their flat-band energy level diagram is reported in Figure 2b. The active layer was chosen for its moderate energy barrier (≈ 0.5 eV) at the cathode/active layer interface so it can be a good model system to test the effect of interlayers.

CILs are deposited by spin-coating a 5 mg mL⁻¹ EtOH solution of CPEs and blends. The CIL/emitting layer interface is preserved during the device fabrication since the emitting layer is processed from chlorobenzene and it's not soluble in EtOH. Non-contact AFM technique (Figure S3, Supporting Information), shows a flat surface with a root mean square roughness (RMS) below 1 nm (Figure S3h, Supporting Information) for all CILs. RMS values of blends are slightly higher than those of P1 and P2, while PF-NBr-EP is as flat as P1 and P2.

First, we tested polymers P1 and P2 separately to verify what effect they have on devices operation. As expected, a sharp increase of performance is observed for devices with respect to OLEDs with simple Ba/Al cathode (OLED0). The incorporation of P1 on the emitting layer led $\approx 17\%$ of increase of OLED1 external quantum efficiency (EQE), from 2.05% of the reference OLED0 to 2.40%. The luminous efficiency (LE) remained unchanged while the turn-on voltage (V_{ON}) shifted from 8 to 10 V (Figure 3 and

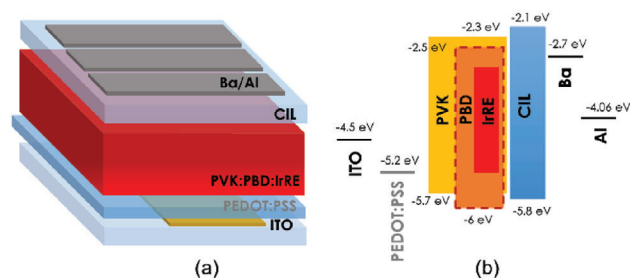


Figure 2. a) Schematic structure of PVK:PBD:IrRE based OLEDs used in the study; b) flat-band energy levels diagram of the materials.

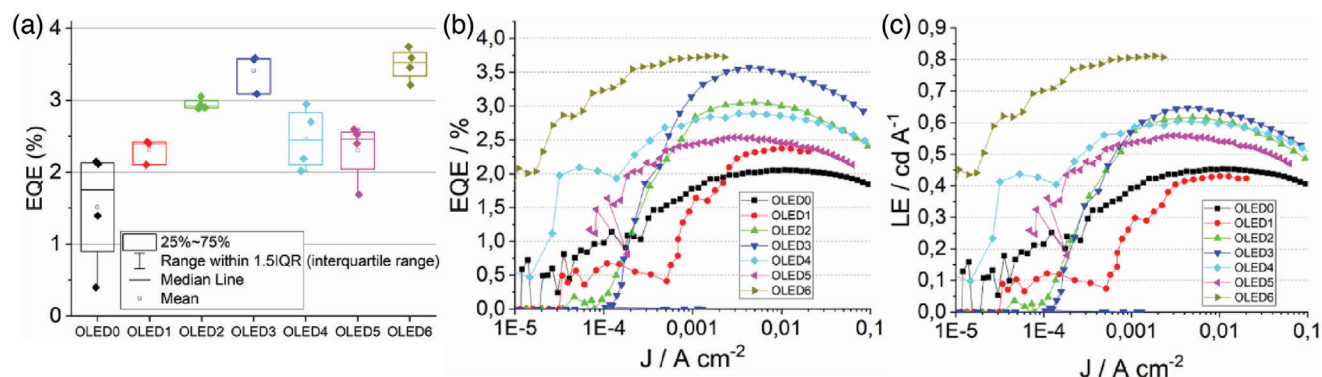


Figure 3. a) EQE values of all OLEDs together with their statistical distribution; b) EQE and c) LE of OLED0-6 as a function of current density (J).

Table 2; Figure S4, Supporting Information). In the case of polymer P2, the improvement of OLED5 was marked even more. The EQE raised from 2.05% to 2.54% (corresponding to 25% of increase), LE from 0.44 to 0.56 cd^{-1} , while V_{ON} remained equal to 8 V (Figure 3 and Table 2; Figure S4, Supporting Information).

Subsequently, we mixed polymers P1 and P2 with weight ratios of 1:0.5, 1:1 and 1:2 (OLED2, 3, 4, respectively). All the mixtures resulted in higher EQE with respect to the reference device without CIL. The best results were achieved in OLED3 with EQE that boosted to 3.57% corresponding to $\approx 75\%$ of increase with respect to OLEDO, LE augmented from 0.45 to 0.65 cd^{-1} and concomitantly the V_{ON} decreased to 6 V from 8 V (Figure 3 and Table 2; Figure S4, Supporting Information). OLED2,4 were not as good as OLED3, but still the improvements were well evident with respect to the OLEDO (Figure 3 and Table 2; Figure S4, Supporting Information) and also to OLED1 and OLED5. These results show that the EP and NBr functionalities actually work synergistically in enhancing OLED performance. The energy barrier for electron injection is properly reduced by shifting Ba/Al work function thanks to the formation of dipoles at the interface.

It is worth to stress that the recorded EL spectra of all the devices did not show any contribution from CIL emission (Figure S5, Supporting Information).

Finally, PF-NBr-EP was employed as a CIL in OLED6. The efficiency was pushed further from OLED3 result, achieving the EQE of 3.74%, LE equal to 0.81 cd^{-1} and low V_{ON} of 6.5 V. The maximal luminance reached 1400 cd^{-2} with $\text{CIE}_{x,y} = (0.69, 0.29)$. The incorporation of the two functionalities on the same poly-

Table 2. Summary of OLEDs performance: turn on voltage (V_{ON}), maximum EQE, maximum luminance (L) and maximum luminous efficiency (LE).

Engineered Ba/Al cathode	V_{ON} [V]	EQE _{MAX} [%]	L_{MAX} (at V) [cd^{-2}]	LE _{MAX} [cd^{-1}]
OLED0 NO CIL	8	2.05	1030 (24)	0.45
OLED1 CIL1	10	2.40	1000 (20)	0.44
OLED2 CIL2	7	3.10	1180 (20)	0.62
OLED3 CIL3	6	3.57	1170 (26)	0.65
OLED4 CIL4	6	2.89	1190 (20)	0.61
OLED5 CIL5	8	2.54	1070 (20)	0.56
OLED6 PF-NBr-EP	6.5	3.74	1400 (20)	0.81

mer backbone in PF-NBr-EP has the further advantage of a more stable morphology and promotes an additional enhancement of OLEDs performance.

Another important consequence of the use of CILs is the peculiar ability of the EP group to effectively graft the polymeric layer onto the aluminum cathode during the top deposition of Al atoms.^[16] This coordination may increase interfacial dipole effect or result in interfacial n-type doping of the PF-EP layer at PF-EP/Al interfaces, further reducing electron injection barrier from Al cathode to the EP-bearing layer.^[16]

Scanning Kelvin probe microscopy is carried out to support this hypothesis by investigating surface energetics of the CILs deposited on Al films (Table 3) and the changes in engineered cathode work functions.

The presence of EP moieties seems to mostly influence the surface potentials (Table 3). A large contact potential difference (CPDs) of $\approx 350\text{--}400$ meV is observed for both CIL5/Al and PF-NBr-EP/Al with respect to bare Al, while P1 apparently leaves Al work function unaffected. CPD values increase (from 140 to 350 meV) from CIL2 to CIL4, accordingly with an increase of EP moieties content. This trend corresponds to a general reduction of energy barrier for electron injection, to a different extent, with the introduction of CIL compared to Al, except for P1.

The reduction of the energy barrier for electron injection creates an opportunity for the manufacturing of OLEDs with the use of a simple aluminum cathode, avoiding the high reactive barium and possibly enhancing the stability in ambient condition.

Table S1 (Supporting Information) presents the performance of devices with different CILs and just Al electrode. A significant decrease of V_{ON} from 15 V for the reference device without

Table 3. Surface potentials measured on CIL-engineered Al cathode.

Sample	Surface potential [eV]
Al	1.13
CIL1/Al	1.12
CIL2/Al	1.27
CIL3/Al	1.32
CIL4/Al	1.38
CIL5/Al	1.53
CIL6/Al	1.48

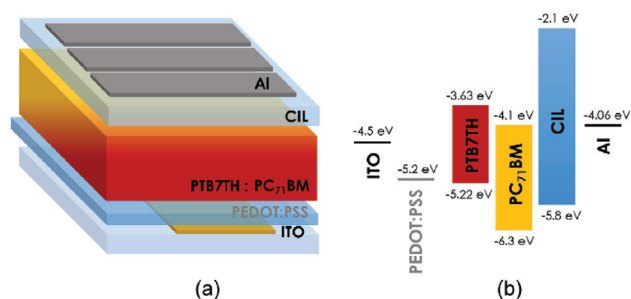


Figure 4. a) Schematic structure of PTB7TH/PC71BM BHJ OSC used in the study; b) flat-band energy levels diagram of the materials.

CIL to 7–8 V voltage range is observed. Luminance plotted versus both applied voltage and current density (Figure S6, Supporting Information) shows that from the same amount of charge, devices with CILs can produce more light. As a final point, corresponding EQE and luminance (Figure S6, Supporting Information), values increased considerably (EQE \approx 2.6–3.04%) with respect to reference OLED (EQE = 1.36%) proving that the use of EP-incorporating CIL could be a way to considerably simplify cathode fabrication.

2.3.2. OSCs

P1, P2, P1/P2 blends and PF-NBr-EP were tested as CIL also in bulk heterojunction (BHJ) solar cells. Herein we have examined conventional BHJ OSCs devices with a structure glass/ITO/PEDOT:PSS/AL/CIL/Al, as shown in **Figure 4**. The AL contains a fullerene derivative, PC₇₁BM (phenyl-C₇₁-butyric acid methyl ester) and PTB7-Th (poly[4,8-bis(5-(2-ethylhexyl)thiophen-2-

yl)benzo[1,2-b;4,5-b']dithiophene-2,6-diyl-alt-(4-(2-ethylhexyl)-3-fluorothieno[3,4-b]thiophene)-(2-carboxylate-2,6-diyl)) (Figure S2, Supporting Information), a low bandgap polymer which, despite a slight batch dependence behavior, is widely used within OSC research for the development of novel functional materials, including non-fullerene acceptors and ILS.^[34]

The CIL thickness is even more critical for OSCs than for OLEDs. For OSCs the CPEs films deposited on top of the AL should be much thinner than in OLEDs. This feature can be explained by considering that in OSCs, electron extraction through interlayer material takes place by charge tunneling. Too thick CILs (>10 nm), beside preserving the interface engineering at the Al electrode, act as electron blocking layer, forming a barrier that hinders charges extraction.^[18,35] As such only very thin layers (\approx 5 nm) have been demonstrated to be successful in enhancing OSCs efficiency.^[26,33]

Therefore, the concentration of all the CILs solutions were fixed at 0.5 mg mL⁻¹ in EtOH solution and, by tuning deposition parameters, films of \approx 4–5 nm were achieved, yielding the best performing device.^[26,29] However, the control of CIL thickness, for film thinner than 10 nm, with a solution process is very hard and introduces unavoidable errors into OSCs performances.

The current density–voltage (*J*–*V*) curves of the OSC1-5 and PF-NBr-EP (OSC6) are reported in **Figure 5a** (and Figure S7, Supporting Information), while the corresponding photovoltaic (PV) parameters are listed in **Table 4** and reported in Figure 5b–f (and Figure S8, Supporting Information). A device without any CIL (OSC0), where the Al electrode was directly evaporated on top of the AL, was taken as a reference. The impact of the CILs in OSC1-5, including OSC0 and OSC6, on the PV parameters is displayed in Figure 5.

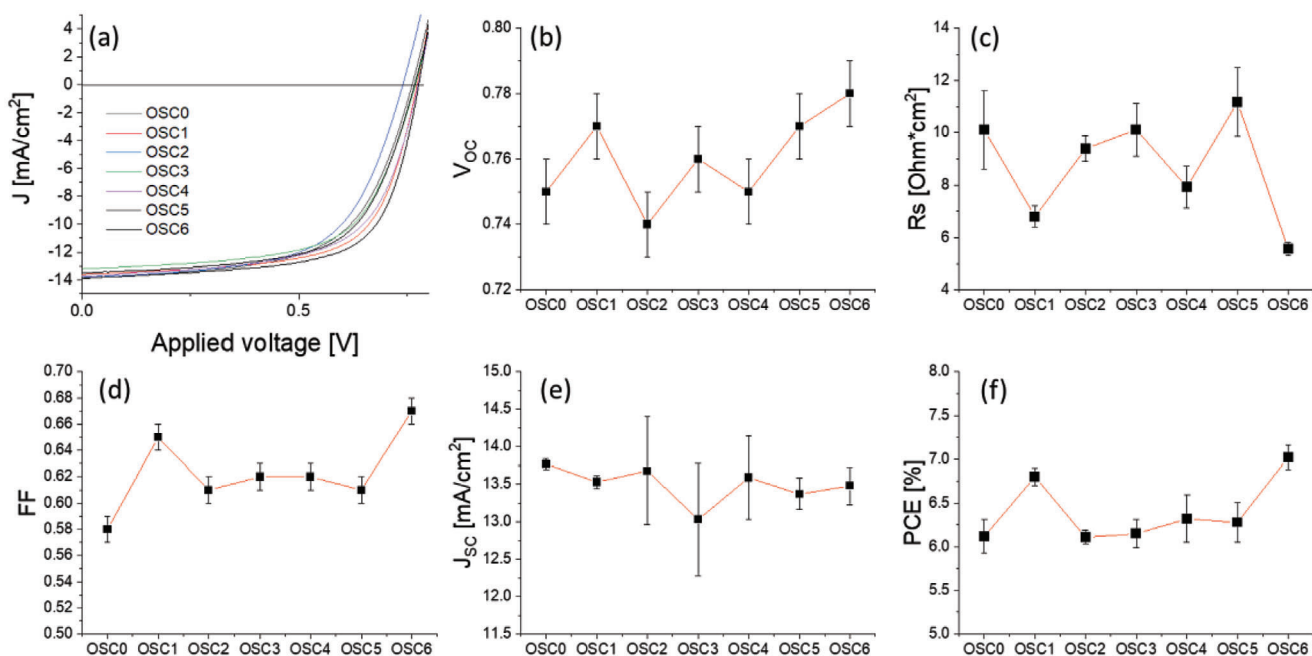


Figure 5. a) *J*–*V* characteristics of PTB7TH:PC71BM-based OSCs under AM 1.5G irradiation at 100mW cm⁻² as a function of P1 (OSC1), d) P2 (OSC5), P1:P2 blends (OSC2-4) and PF-NBr-EP interlayers (OSC6). The device without CIL (OSC0) is reported as reference; b–f) average PV parameters as a function of the IL.

Table 4. PV parameters of PTB7TH:PC71BM-based OSCs under AM 1.5G irradiation (100 mW cm^{-2}) with different interlayers. Parameters are averaged over eight devices (maximum values are reported for V_{oc} , FF, J_{sc} , PCE). Series resistances (R_s) are derived from the J - V characteristic as the reverse of the linear fitting slope in the range of voltage around the corresponding V_{oc} value. J_{sc}^{EQE} is derived from EQE spectra.

Sample	Engineered LiF/ Al cathode	V_{oc} (V_{oc}^{MAX}) [V]	FF (FF^{MAX})	J_s (J_{sc}^{MAX}) [mA cm^{-2}]	PCE (PCE^{MAX}) [%]	R_s [$\Omega \text{ cm}^2$]	J_{sc}^{EQE} [mA cm^{-2}]
OSC0	none	0.75 ± 0.01 (0.77)	0.58 ± 0.01 (0.60)	13.77 ± 0.07 (13.86)	6.12 ± 0.19 (6.40)	10.11 ± 1.50	14.17
OSC1	CIL1	0.77 ± 0.01 (0.78)	0.65 ± 0.01 (0.66)	13.53 ± 0.09 (13.61)	6.80 ± 0.10 (6.92)	6.80 ± 0.42	14.08
OSC2	CIL2	0.74 ± 0.01 (0.76)	0.61 ± 0.01 (0.61)	13.68 ± 0.72 (13.79)	6.11 ± 0.08 (6.20)	9.40 ± 0.50	14.68
OSC3	CIL3	0.76 ± 0.01 (0.77)	0.62 ± 0.01 (0.63)	13.03 ± 1.15 (13.20)	6.15 ± 0.16 (6.38)	10.12 ± 1.00	13.68
OSC4	CIL4	0.75 ± 0.01 (0.77)	0.62 ± 0.01 (0.63)	13.59 ± 0.56 (13.72)	6.32 ± 0.27 (6.69)	7.93 ± 0.80	14.65
OSC5	CIL5	0.77 ± 0.01 (0.78)	0.61 ± 0.01 (0.63)	13.37 ± 0.21 (13.52)	6.28 ± 0.23 (6.55)	11.18 ± 1.32	14.29
OSC6	PF-NBr-EP	0.78 ± 0.01 (0.79)	0.67 ± 0.01 (0.68)	13.48 ± 0.25 (13.88)	7.02 ± 0.14 (7.20)	5.56 ± 0.26	14.41

Unlike OLEDs, OSC1 exhibits higher efficiency with respect to OSC2-5. In OSC1, the insertion of P1 CIL induces an improvement of the PV performance when compared to the OSC0. This is due to a gain of the V_{oc} and FF parameters that is the typical signature of an effective engineering of the electrodes that improves the charge extraction of the photogenerated charges.^[36]

When going to OSC5, there is an obvious reduction of the FF and a relevant increase of the series resistance (R_s), reaching similar, or even higher, values to the reference device OSC0. Upon blending P1 and P2, the FF values of OSC2-4 remain lower, while the R_s values are higher when compared to OSC1. This suggests poor electrical contact, due to barrier at the CIL/AL interface that is hindering the extraction of the photogenerated electrons from the cathode.

Furthermore, our results show that insertion of the PF-NBr-EP interlayer is boosting the PV performance of OSC6, showing the higher V_{oc} and FF and lower R_s among these CILs devices series.

To discuss the above results one should consider that, as mentioned above, P2 is much more hydrophilic than P1 (Figure 1 and Figure S1, Supporting Information). For this reason, de-wetting issues may occur and a quite complicated situation in the P1/P2 blends may arise. This makes the control of the CIL2-5 thickness furthermore complicated.

Moreover, according to the AFM images (Figure 6a–g), CIL2-4 show a higher RMS with respect to CIL1,5 and PF-NBr-EP (Figure 6h). Even if film morphology does not explain the variation of OSCs performance by RMS fluctuations, it can be seen as an indication that phase segregation within blended CPE films deposited on PTB7TH:PC71BM may occur.

One of the reasons to explain the best performances of P1 and PF-NBr-EP CILs, is the presence of the NBr groups in both polymers. It has been reported that NBr interfacial n-doping of the fullerene is an important phenomenon that minimize the contact resistance at the active layer/cathode interlayer.^[23] This helps in mitigating the need of having an extremely precise control of the CIL thickness when using P1 and PF-NBr-EP.^[2,35]

3. Conclusion

In conclusion, by analysing the effect of NBr and EP bearing CPEs (called P1 and P2 respectively), used as CIL, and their blends on the performance of OLEDs and OSCs, we wanted to support our choice of designing and developing the bifunctional

PF-NBr-EP CPE, earlier successfully incorporated as a CIL to boost performance of diverse electronic and optoelectronic devices.

We prepared blends of the two known polymers (P1 and P2) each of which bears the individual EP or NBr groups to show that 1) the combination of the two moieties can lead to greater beneficial effect than the use of the single ones, and 2) to evaluate what could be the more effective EP/NBr ratio for both types of devices.

Different types of devices, i.e., OLEDs and OSCs, due to their peculiar working mechanisms, need different optimized CIL thickness. We took this into account by tuning both CPEs solution concentration and process parameters to form films with precise thickness.

OLEDs embedding blend P1 and P2 as CIL exhibited improved performance in term of EQE with respect to parent polymers. The 1:1 ratio resulted to be more efficient thanks to the combined effect of EP and NBr in mitigating electron injection barrier. The affinity of EP to Al allowed us to avoid Ba application in cathode fabrication.

EP groups alone are not as beneficial for OSCs performance as for OLEDs and due to their hydrophilic nature de-wetting issues may occur once blended with P1. On the other hand, NBr interfacial n-doping of the fullerene is most probably a dominant phenomenon that minimizes the contact resistance at the active layer/cathode interlayer leading to more performing OSCs.

The incorporation of EP and NBr moieties into a single material, i.e., PF-NBr-EP, that maintained both the specific characteristics of the starting polymers, besides the simplification in device fabrication process, has proven to be effective in boosting performance of different types of devices like OLEDs, nanocrystal LEDs, OSCs, OLETs.

The development of such universal-type CIL materials is projected to play a significant and enabling role in eco-sustainable process for fabricating electronic and optoelectronic devices.

4. Experimental Section

Chemicals: Poly[(2,7-(9,9'-dioctyl)fluorene)-alt-(2,7-(9,9'-bis(6"-tri-methylammonium bromide)hexyl)-fluorene)] (P1) was synthesized according to the literature.^[25] Poly[9,9-bis(6'-diethoxyphosphoryl)hexyl]-fluorene] (P2) was synthesized using a modified literature procedure

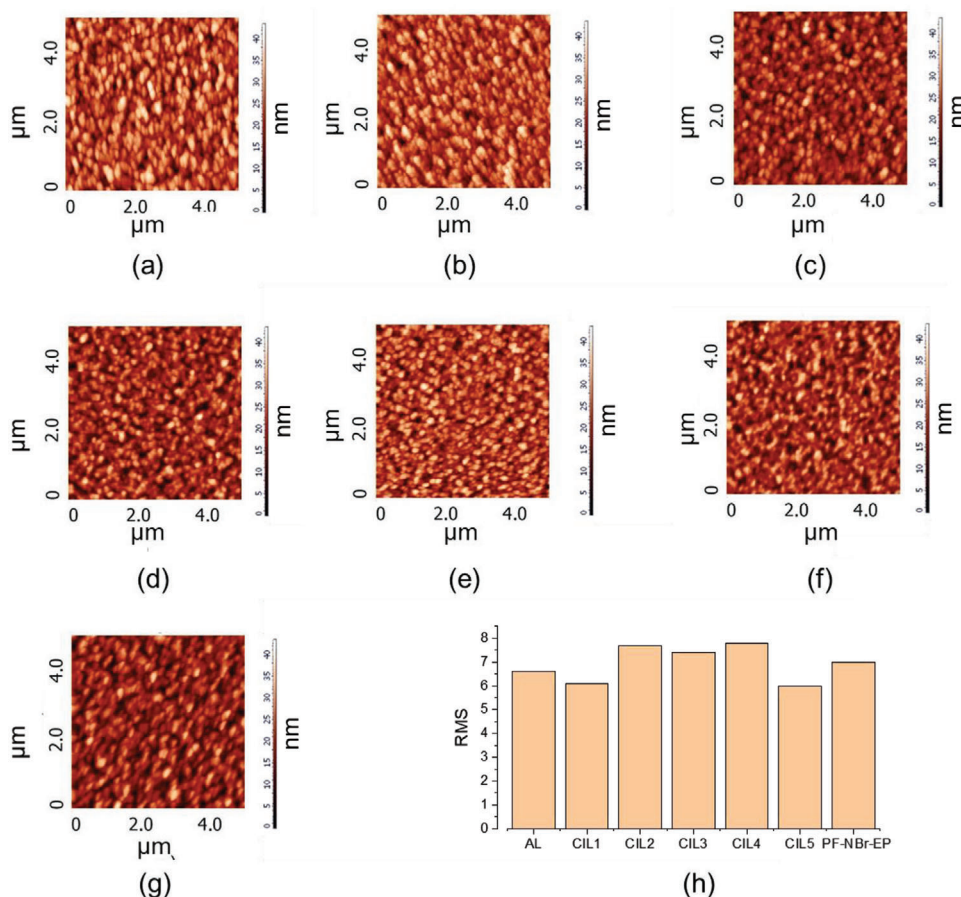


Figure 6. 5 μm x 5 μm non-contact AFM height images of CILs deposited on the OSC active layer. a) uncovered AL, b) CIL1, c) CIL2, d) CIL3, e) CIL4, f) CIL5, g) PF-NBr-EP, and h) RMS values of different CILs deposited on OSCs AL.

according to the previous work.^[27] The PF-NBr-EP namely poly[(2,7-(9,9'-bis(6'-diethoxyphosphorylhexyl)-fluorene)-alt-(2,7-(9,9'-bis(6'-trimethylammonium bromide)hexyl)-fluorene))] synthesis was performed following a recently published paper.^[24] All chemicals and reagents were used as received from commercial sources without further purification. Solvents for chemical synthesis were purified according to standard procedures. All chemical reactions were carried out under an inert atmosphere.

Characterization and Devices: Contact angle measurements were collected via the sessile drop method using a CAM 200 instrument (KSV Ltd.), which utilizes video capture and subsequent image analysis. Atomic Force Microscopy (AFM) was performed with commercial equipment (AFM NT-MDT NTEGRA) in tapping mode with a cantilever NSG10 operating at a typical resonance frequency of 140–390 kHz.

For the assembling of solar cells, glass ITO (Kintec) 15 Ω sq^{-1} substrates were mechanically cleaned with peeling tape and paper with acetone and then were washed in a sonic bath at 50 $^{\circ}\text{C}$ for 10 min sequentially with water, acetone, and isopropanol. After drying plasma treatment in the air was used to enhance ITO wettability for the next deposition. PEDOT:PSS was filtered on a 0.45 μm nylon filter, spin-coated in the air at 2500 rpm for 60 s and finally stored in a glovebox and annealed at 150 $^{\circ}\text{C}$ for 10 min. The device assembly was then performed in glovebox. The active layer was composed by a blend of 1:1.5 wt./wt. of PTB7TH:PC71BM dissolved in 1-chlorobenzene at a total concentration of 20 mg mL^{-1} . The solution was stirred for 12 h on a hotplate in glovebox at 60 $^{\circ}\text{C}$; subsequently, a 1.8% v/v of 4-anisaldehyde was added to the blend solution. The active layer was spin-coated from the warm solution at 2000 rpm for

60 s, which results in a thickness of 90 nm; then, the device was placed on a 65 $^{\circ}\text{C}$ hotplate for 15 min to help solvent evaporation. 60 μL of CILs ethanol solutions (at 0.5 mg mL^{-1}) were dropped on the rotating device at 4000 rpm for 60 s. Finally, 100 nm thick aluminum electrode was evaporated on the top of the device through a shadow mask under a pressure of 2×10^{-6} mbar. Active area of the devices was 6.1 mm^2 .

OLEDs were assembled with the conventional structure glass/ITO/PEDOT:PSS/active/interlayer/Ba/Al. The glass ITO 15 Ω sq^{-1} (Kintec) was cleaned by following the procedure reported for solar cells. A 35 nm thick PEDOT:PSS layer was spin-coated and consequently annealed at 150 $^{\circ}\text{C}$ for 10 min inside a nitrogen-filled glovebox. The emitting layer was composed by commercially available compounds. Hole transporting PVK was blended with electron transporting PBD and Ir(III) complex (IrRE). A 20 mg mL^{-1} degassed chlorobenzene solution was spincoated at 600 rpm. CILs were spin-coated from a 5 mg mL^{-1} EtOH solution at 4000 rpm. Barium (6 nm)/Aluminum cathode (100 nm) was finally evaporated on top of the organic layers as reported above. There were four devices on a single substrate, each with an active area of 6.1 mm^2 .

Current density–voltage measurements on solar cells were performed directly in the glovebox where the solar cells were assembled, with a Keithley 2602 source meter, under dark or under an AM 1.5 G solar simulator (ABET 2000). The incident power, measured with a calibrated photodiode, was 100 mW cm^{-2} . The external quantum efficiency (EQE) spectral responses were recorded by dispersing an Xe lamp through a monochromator, using a Si solar cell with a calibrated spectral response to measure the incident light power intensity at each wavelength. The devices were taken outside the glovebox for the EQE measurements, after mounting

them on a sealed cell to avoid moisture and oxygen exposure. Current density-luminance-voltage measurements of OLEDs were performed in the glovebox with a Keithley 2602 source meter and Konica–Minolta LS-150. Electroluminescence and Photoluminescence spectra were recorded by means of modified Horiba Fluorolog system.

Supporting Information

Supporting Information is available from the Wiley Online Library or from the author.

Acknowledgements

U.G., G.S. and C.B. would like to thank the Italian University and Research Ministry PRIN Project 20172M3K5N for financial support.

Conflict of Interest

The authors declare no conflict of interest.

Data Availability Statement

The data that support the findings of this study are available in the supplementary material of this article.

Keywords

cathode interfacial layers, conjugated polyelectrolytes, fluorenes, OLEDs, organic solar cells

Received: April 27, 2023

Revised: July 6, 2023

Published online:

- [1] Y. Zhou, C. Fuentes-Hernandez, J. Shim, J. Meyer, A. J. Giordano, H. Li, P. Winget, T. Papadopoulos, H. Cheun, J. Kim, M. Fenoll, A. Dindar, W. Haske, E. Najafabadi, T. M. Khan, H. Sojoudi, S. Barlow, S. Graham, J.-L. Brédas, S. R. Marder, A. Kahn, B. Kippelen, *Science* **2012**, 336, 327.
- [2] R. Sorrentino, E. Kozma, S. Luzzati, R. Po, *Energy Environ. Sci.* **2021**, 14, 180.
- [3] K. Müllen, U. Scherf, *Macromol. Chem. Phys.* **2023**, 224, 2200337.
- [4] N. Aizawa, Y.-J. Pu, M. Watanabe, T. Chiba, K. Ideta, N. Toyota, M. Igarashi, Y. Suzuri, H. Sasabe, J. Kido, *Nat. Commun.* **2014**, 5, 5756.
- [5] F. Huang, H. Wu, Y. Cao, *Chem. Soc. Rev.* **2010**, 39, 2500.
- [6] Y. Wu, Y. Liu, T. Emrick, T. P. Russell, *Prog. Polym. Sci.* **2020**, 103, 101222.
- [7] J. H. Seo, A. Gutacker, Y. Sun, H. Wu, F. Huang, Y. Cao, U. Scherf, A. J. Heeger, G. C. Bazan, *J. Am. Chem. Soc.* **2011**, 133, 8416.
- [8] Y. Zhao, Z. Xie, C. Qin, Y. Qu, Y. Geng, L. Wang, *Sol. Energy Mater. Sol. Cells* **2009**, 93, 604.
- [9] Luo, J., Wu, H., He, C., Li, A., Yang, W., Cao, Y., *Appl. Phys. Lett.* **2009**, 95, 043301.
- [10] S.-H. Oh, S.-I.n Na, J. Jo, B. Lim, D. Vak, D.-Y.u Kim, *Adv. Funct. Mater.* **2010**, 20, 1977.
- [11] Z. He, C. Zhong, S. Su, M. Xu, H. Wu, Y. Cao, *Nat. Photonics* **2012**, 6, 591.
- [12] K. Zhang, C. Zhong, S. Liu, C. Mu, Z. Li, H.e Yan, F. Huang, Y. Cao, *ACS Appl. Mater. Interfaces* **2014**, 6, 10429.
- [13] Z. He, C. Zhong, X. Huang, W.-Y. Wong, H. Wu, L. Chen, S. Su, Y. Cao, *Adv. Mater.* **2011**, 23, 4636.
- [14] T. Yang, M. Wang, C. Duan, X. Hu, L. Huang, J. Peng, F. Huang, X. Gong, *Energy Environ. Sci.* **2012**, 5, 8208.
- [15] A. Krishna, A. V. Lunchev, A. C. Grimsdale, in *Suzuki Polycondensation, in Synthetic Methods for Conjugated Polymers and Carbon Materials*, John Wiley & Sons, Hoboken, NJ, USA **2017**, pp. 59–95.
- [16] B. Zhang, C. Qin, X. Niu, Z. Xie, Y. Cheng, L. Wang, X. Li, *Appl. Phys. Lett.* **2010**, 97, 043506.
- [17] Zhou, G., Qian, G., Ma, L., Cheng, Y., Xie, Z., Wang, L., Jing, X., Wang, F., *Macromolecules* **2005**, 38, 5416.
- [18] B. H. Lee, I. H. Jung, H. Y. Woo, H.-K. Shim, G. Kim, K. Lee, *Adv. Funct. Mater.* **2014**, 24, 1100.
- [19] Z. Hu, Z. Zhong, Y. Chen, C. Sun, F. Huang, J. Peng, J. Wang, Y. Cao, *Adv. Funct. Mater.* **2016**, 26, 129.
- [20] Z. He, H. Wu, Y. Cao, *Adv. Mater.* **2014**, 26, 1006.
- [21] Z. Hu, K. Zhang, F. Huang, Y. Cao, *Chem. Commun.* **2015**, 51, 5572.
- [22] T. Li, Z. Chen, Y. Wang, J. Tu, X. Deng, Q. Li, Z. Li, *ACS Appl. Mater. Interfaces* **2020**, 12, 3301.
- [23] C.-Z. Li, C.-C. Chueh, F. Ding, H.-L. Yip, P.-W. Liang, X. Li, A. K.-Y. Jen, *Adv. Mater.* **2013**, 25, 4425.
- [24] U. Giovanella, M. Pasini, M. Lorenzon, F. Galeotti, C. Lucchi, F. Meinardi, S. Luzzati, B. Dubertret, S. Brovelli, *Nano Lett.* **2018**, 18, 3441.
- [25] A. Castelli, F. Meinardi, M. Pasini, F. Galeotti, V. Pinchetti, M. Lorenzon, L. Manna, I. Moreels, U. Giovanella, S. Brovelli, *Nano Lett.* **2015**, 15, 5455.
- [26] F. Carulli, G. Scavia, E. Lassi, M. Pasini, F. Galeotti, S. Brovelli, U. Giovanella, S. Luzzati, *J. Colloid Interface Sci.* **2019**, 538, 611.
- [27] M. Prosa, E. Benvenuti, M. Pasini, U. Giovanella, M. Bolognesi, L. Meazza, F. Galeotti, M. Muccini, S. Toffanin, *ACS Appl. Mater. Interfaces* **2018**, 10, 25580.
- [28] X. Niu, C. Qin, B. Zhang, J. Yang, Z. Xie, Y. Cheng, L. Wang, *Appl. Phys. Lett.* **2007**, 90, 203513.
- [29] F. Carulli, W. Mróz, E. Lassi, C. Sandionigi, B. Squeo, L. Meazza, G. Scavia, S. Luzzati, M. Pasini, U. Giovanella, F. Galeotti, *Chem. Pap.* **2018**, 72, 1753.
- [30] U. Giovanella, M. Pasini, S. Destri, W. Porzio, C. Botta, *Synth. Met.* **2008**, 158, 113.
- [31] M. Pasini, U. Giovanella, P. Betti, A. Bolognesi, C. Botta, S. Destri, W. Porzio, B. Vercelli, G. Zotti, *ChemPhysChem* **2009**, 10, 2143.
- [32] U. Giovanella, M. Pasini, C. Botta, **2016** in *Applied Photochemistry: When Light Meets Molecules* (Eds: G. Bergamini, S. Silvi), Springer, Cham, pp. 145–196.
- [33] C. Duan, K. Zhang, C. Zhong, F. Huang, Y. Cao, *Chem. Soc. Rev.* **2013**, 42, 9071.
- [34] A. R. Tetreault, M.-T. Dang, T. P. Bender, *Synth. Met.* **2022**, 287, 117088.
- [35] C. Sun, Z. Wu, Z. Hu, J. Xiao, W. Zhao, H.-W. Li, Q.-Y. Li, S.-W. Tsang, Y.-X. Xu, K. Zhang, H.-L. Yip, J. Hou, F. Huang, Y. Cao, *Energy Environ. Sci.* **2017**, 10, 1784.
- [36] G. Zhang, F. R. Lin, F. Qi, T. Heumüller, A. Distler, H.-J. Egelhaaf, N. Li, P. C. Y Chow, C. J. Brabec, A. K.-Y. Jen, H.-L. Yip, *Chem. Rev.* **2022**, 122, 14180.